

Molecular dynamics study of the interactions of incident N or Ti atoms with the TiN(001) surface

Zhenhai Xu^{1,2,3}, Quanren Zeng³, Lin Yuan¹, Yi Qin³, Mingjun Chen², Debin Shan^{1*}

¹ National Key Laboratory for Precision Hot Processing of Metals & School of Materials Science and Engineering, Harbin Institute of Technology, Harbin 150001, China

² School of Mechatronics Engineering, Harbin Institute of Technology, Harbin 150001, China

³ Centre for Precision Manufacturing, Department of Design, Manufacture and Engineering Management, The University of Strathclyde, Glasgow G1 1XJ, UK

*Corresponding authors. E-mail: d.b.shan@gmail.com

Abstract

The interaction processes between incident N or Ti atoms and the TiN(001) surface are simulated by classical molecular dynamics based on the second nearest-neighbor modified embedded-atom method potentials. The simulations are carried out for substrate temperatures between 300–700 K and kinetic energies of the incident atoms within the range of 0.5–10 eV. When N atoms impact against the surface, adsorption, resputtering and reflection of particles are observed; several unique atomic mechanisms are identified to account for these interactions, in which the adsorption could occur due to the atomic exchange process while the resputtering and reflection may simultaneously occur. The impact position of incident N atoms on the surface plays an important role in determining the interaction modes. Their occurrence probabilities are dependent on the kinetic energy of incident N atoms but independent on the substrate temperature. When Ti atoms are the incident particles, adsorption is the predominant interaction mode between particles and the surface. This results in the much smaller initial sticking coefficient of N atoms on the TiN(001) surface compared with that of Ti atoms. Stoichiometric TiN is promoted by N/Ti flux ratios larger than one.

Keywords: TiN; atomic deposition; adsorption; resputtering; reflection; molecular dynamics.

1. Introduction

The B1-structured TiN possesses both ceramic and metallic characteristics, resulting in its outstanding mechanical and distinctive physical properties, such as good resistance to wear and corrosion, golden color, low electrical resistivity, high thermal stability, high reflectance in the red and infrared, and desirable biocompatibility. Therefore, TiN coatings and films have wide protective or functional applications such as wear-resistant hard coatings on cutting tools, corrosion-resistant coatings on mechanical parts, decorative overlayers on end-products, diffusion barriers in microelectronics devices, anti-reflective layers on optical components, and biomedical protective coatings on orthopedic and dental implants [1–6]. Their performances closely depend on their microstructures, which are mainly determined by the production conditions. TiN coatings and films are usually produced by various physical vapor deposition (PVD) techniques, where the relationship among deposition parameters, microstructures and performances has always been the focus of extensive experimental researches. However, the

This is a pre-copyedited, author-produced PDF of an article accepted for publication in **Applied Surface Science** (2016, 360: 946–952) following peer review. The formal publication is available at Elsevier via <http://dx.doi.org/10.1016/j.apsusc.2015.11.090>.

Publication statuses: Accepted 7 Nov. 2015, Available online 18 Nov. 2015, Published 1 Jan. 2016.



© 2015. This manuscript version is made available under the CC-BY-NC-ND 4.0 license <http://creativecommons.org/licenses/by-nc-nd/4.0/>

results are sometimes incompatible, probably due to the complexity of the PVD process resulting in the mutual effects of different deposition parameters, e.g., a variation in one deposition parameter will unintentionally change others [7]. Furthermore, the essential reason is the lack of the fundamental understanding of the TiN film growth process, which is intrinsically a non-equilibrium phenomenon governed by the interplay of thermodynamic driving force and kinetic atomic diffusion and adsorption processes on surfaces. The current atomic-level experimental techniques, such as low energy electron diffraction and scanning tunneling microscopy, have allowed the direct visualization of atomic structures of surfaces, but they cannot resolve the kinetic process of atoms at picosecond scale [8, 9]; therefore, atomistic simulation has become a valuable complementary method for the study of film growth at atomic scale. Films could grow by atomic units [10] or nanometer-sized clusters [11] during the PVD, which therefore is generally simplified as an atomic deposition process [12] or an atomic cluster deposition process [13]. PVD processes have been modeled via classical molecular dynamics (CMD) simulations based on these two models [12–18].

The TiN film growth during the PVD is primarily attributed to the fluxes of atomic N and Ti reacting on the surface of substrate [10]. Therefore, it can be regarded as an atomic deposition process, where the overlay material is deposited atom-by-atom. Density functional calculation by Gall *et al.* shows that the N, Ti adatoms and TiN_x ad molecule ($x=1-3$) are the primary diffusing species, and their diffusion behavior are affected by the incident N/Ti flux ratio [19]. Sangiovanni *et al.* [9, 20] investigated the transport kinetics of the N, Ti adatoms and TiN_x ad molecule ($x=1-3$) on the TiN(001) surface using MD simulations, and their results indicate that the dominant N-containing ad molecule species and the film growth modes depend upon the incident N/Ti adsorption ratio. These investigations were mainly focused on identifying the diffusing species and their transport processes on the TiN surface, and also found the important role of the N/Ti adsorption ratio on the film growth. Hence, the CMD study of the interaction processes between incident atoms and the substrate surface is required to allow one to understand the effect of the incident fluxes of atomic N and Ti on the resulting N/Ti adsorption ratio. In addition, the sticking coefficient of incident atoms calculated by CMD simulations provides much convenience compared with its challenging experimental measurement [21, 22], and the value can serve as the input parameter for some analytic deposition models and directly guide the deposition parameter selection [23]. Most CMD studies of the film deposition do not cover this field due to the nearly complete adsorption of incident metal atoms and clusters on the substrate surface, while the interaction between the incident light N atom and the substrate surface is significantly different. An atomic insight into this interaction will deepen the understanding of the TiN film growth, and also provides an instance of studying the interaction behavior of other incident light atoms or gas molecules on solid surfaces by CMD simulations.

Our previous research using an atomic deposition model has revealed the growth mechanism of the TiN film [12]. In this work, we use the similar CMD model and the same interatomic potentials to investigate the interactions between incident N or Ti atoms and the TiN(001) surface. The different atomistic response mechanisms of these interaction processes are revealed, and the initial sticking coefficients of atomic N or Ti on the TiN(001) surface are calculated. The effects of the substrate temperature and the kinetic energy of incident atoms on them are discussed.

2. Computational method

The interatomic potential is a key element to any CMD simulation which determines the feasibility and reliability of the CMD simulation. The second nearest-neighbor modified embedded-atom method (2NN MEAM) considers the directivity of bonds and the interaction between the 2NN atoms, and contains the universal Ziegler–Biersack–Littmark repulsive interaction [24] accounting for the interatomic collision at close separation. Therefore, it is suitable to describe the atomic interaction process of incident atoms with surfaces. The 2NN MEAM potential parameters for Ti, N and Ti–N are taken from Kim *et al.* [25], Lee *et al.* [26] and our previous work [12]. The cutoff distance r_c of all potentials is 4.8 Å, which is between the third and fourth nearest-neighbor distances of the hexagonal close packed Ti crystal.

The CMD model in Fig. 1 are used to resolve the interaction process between incident atoms and the TiN(001) surface. The substrate is created from the B1 crystal structure with the x , y , and z axes corresponding to the crystallographic directions [100], [010] and [001]. Its dimensions are $5a_T \times 5a_T \times 5a_T$, where a_T is the lattice constant of TiN at temperature T and its values were taken from our previous work [12]. The substrate is periodic along x and y directions, so it can be regarded as an infinite slab in the x - y plane. The substrate is divided into three regions: the bottom three layers of atoms are fixed to avoid the substrate drift due to the momentum transfer from incident atoms; the Nosé–Hoover thermostat is applied to the middle region to simulate the approximately isothermal condition under which the film growth usually occurs; the top two layers of atoms are free to enable their interactions with incident atoms. The substrate is relaxed for 20 ps to reach the equilibrium state at T . Then an atomic impact process is initiated by injecting one N or Ti atom from an initial height H above the substrate surface and a random site in the x - y incident plane, followed by the whole system relaxation for another 2 ps. Here, H is 0.1 Å larger than r_c to avoid the effect of the substrate surface on the incident atom before the injection, and also to make the interaction between them immediately occur after the injection to save the computational time. The incident atom is assigned an initial kinetic energy E_k and the normal motion direction towards the substrate surface. Within the second relaxation period if any atom attempts to move through a virtual wall above the incident plane with a distance of 0.1 Å, the incident atom is considered as un-adsorbed, otherwise it is considered as adsorbed. One impact cycle is terminated by this identification, and the next cycle starts by injecting one atom with the same kinetic energy from another random location in the same x - y incident plane towards another substrate undergoing the same initial relaxation. For each species of incident atom 500 cycles are performed to finish one simulation. The numbers of the total cycles and adsorption events are accumulated as N_{inc} and N_{ads} , respectively. The initial sticking coefficient, which describes the probability of adsorption of incident atoms on the surface at the zero coverage, could be defined as:

$$S_{00} = N_{\text{ads}} / N_{\text{inc}} \quad (1)$$

The interaction processes of N and Ti on the TiN(001) surface are simulated when $T = 300$ – 700 K and $E_k = 0.5$ – 10 eV, which are within typical operational conditions of sputtering deposition for TiN films [19, 27]. All simulations are performed using the open source code LAMMPS [28] including the MEAM module with input parameters set as $\text{ialloy} = 0$ and $\text{ibar} = 3$. The integration time step is 1 fs. The velocity Verlet algorithm is used to solve the motion equations of atoms. The atomic configurations are visualized by the free software AtomEye [29].

3. Results and discussion

3.1. Interactions of incident N atoms on the TiN(001) surface

The impact of energetic particles on a solid surface could result in adsorption, sputtering and reflection. All these interaction processes occur during the impact of incident N atoms with the TiN(001) surface, furthermore three unique atomic mechanisms as well as three conventional mechanisms are observed to be responsible for these processes. They are illustrated by the time resolved impact processes under the incident condition of $T = 500$ K and $E_k = 10$ eV as shown in Fig. 2 (the corresponding animations are supplied as Supplementary Material available with this article online). The left subfigures show the atomic configurations of the top partition of the substrate and a flying incident atom when the impact is initiated at $t = 0$ fs, where the rectangles restrict the observed spaces for the right series of smaller subfigures. Two different colored rectangles on the left subfigures in Fig. 2(a)–(d) indicate the change of the observed spaces for the right subfigures, and the specific observed space of each subfigure can be determined by its area. Each series of small subfigures arranging from left to right and then from top to bottom resolve the impact process with the time elapse. The observation time step Δt of the small subfigures in Fig. 2(a) is 10 fs, and the values of Δt_{obs} are 10 fs and 15 fs for the first row and the second to the third rows of the small subfigures in Fig. 2(b), respectively. The observation moment of each small subfigure in Fig. 2(c)–(f) is explicitly marked. The odd rows of small subfigures in Fig. 2(c)–(f) are orthographically viewed as the following even rows of small subfigures with only substrate surface atoms and incident atoms, where the location evolution of the incident atom and surface atoms in the incident direction can be distinctly observed.

Fig. 2(a) shows the conventional direct adsorption process of the incident N atom from the gas phase on the TiN(001) surface. The incident N atom gradually approaches the surface until $t = 60$ fs; then it penetrates into the surface and is trapped at the location near the lattice site of the surface atom N1. At $t = 70$ fs the incident atom begins to move out with a reverse velocity component vertical to the surface due to the recoil force effect from the substrate. Since the large fraction of the kinetic energy of the incident atom has been transferred to the substrate during the impact and the drag of N1 on the incident atom is strong, the incident atom exhausts its energy of escaping from the surface and the escaping height reaches the limit at $t = 190$ fs. Then the incident atom is gradually pulled back until adsorbed on the surface, and then oscillates around N1 in $t = 240$ –1000 fs. The adsorbed atom finally rests in a *three-fold* position at the center of a triangle formed by a N terrace atom and the two nearest Ti surface atoms, which has been proved to be the dynamic equilibrium site of the N adatom on the TiN(001) surface by Sangiovanni *et al.* [30]. Fig. 2(b) shows another unique adsorption process. In $t = 0$ –60 fs the incident atom approaches and then penetrates the substrate surface in the same way above to occupy the lattice site of the surface atom N2 together with N2. In $t = 60$ –80 fs the incident atom gradually occupies the surface lattice site exclusively, while N2 is ejected onto the surface since it achieves the large fraction of the kinetic energy of the incident atom and is also recoiled by other substrate atoms. This process is generally called the atomic exchange, which has contributed to explain the interfacial mixing phenomena during the Ni/Cu/Ni multilayer growth, the deposition of Au on the Ag(110) surface and the deposition of Pt on the Au(100) surface [31–33]. After $t = 80$ fs the adsorption process of N2 replays the similar scenario with that illustrated in Fig. 2(a) except that N2 becomes the adsorbed atom while the incident atom becomes the surface atom. It indicates that the adsorption process can

proceed by the atomic exchange mechanism. Fig. 2(c) shows that an atomic exchange event occurs between the incident atom and the surface atom N3 in $t = 0\text{--}90$ fs, but due to the collision N3 achieves enough kinetic energy and appropriate momentum to keep the outward motion after $t = 90$ fs, finally N3 escapes from the surface into the gas phase. This is the conventional resputtering process of the surface atom induced by the incident atom. Fig. 2(d) shows the conventional reflection process of the incident atom. The incident atom retains enough kinetic energy and appropriate momentum to escape from the surface after its collision with the surface atom Ti1, moving into the gas phase at $t = 130$ fs, while Ti1 finally returns its original dynamics equilibrium site after a significant oscillation induced by the collision. Fig. 2(e) shows a unique process of the reflection and resputtering simultaneously occurring in an impact process, resulting in a pair of separate N atoms leaving off the surface. The incident atom is reflected after the collision with the surface atom N4, while N4 is knocked below its lattice site. Then N4 is also resputtered into the gas phase due to the significant recoil force mainly from the Ti atom below N4. The pair of atoms finally moves along two different directions off the surface. Fig. 2(f) shows another mechanism responsible for the simultaneous sputtering and reflection process. The incident atom and the impacted surface N atom are reflected and resputtered in a short time interval, and the former has an additional drag effect on the latter, resulting in the formation of a N₂ molecule which finally moves away from the surface. This scenario is consistent with the *ab initio* MD result [30].

In summary, the impact of an incident N atom with the TiN(001) surface could result in adsorption, resputtering and reflection due to the complicated collision response of the incident atom and the substrate atoms. These interaction processes could proceed by several different atomic mechanisms, which mainly depend on the kinetic energy and momentum transfers between the incident N atom and the TiN(001) surface. The incident atom will get trapped if it loses enough kinetic energy to the substrate, and finally it is adsorbed on the surface directly or occupies the lattice site of the surface N atom by the atomic exchange mechanism, while that surface N atom is adsorbed on the surface or is resputtered into the gas phase with appropriate momentum; otherwise the incident atom will be reflected, or at the same time one surface N atom will also be resputtered. This pair of N atoms could move away from the surface in the mode of two separate individuals or a N₂ molecule.

In order to reveal the correlation of atomic interaction with the impact location of incident atoms on the TiN(001) surface, the initial positions in the x - y plane of all 500 incident atoms for one simulation are projected onto the same substrate surface as shown in Fig. 3(a). The atoms in the top two layers of the substrate are plotted in their lattice sites. The incident atoms are marked as crosses, and colored by their atomic interactions with the substrate surface including the adsorption, resputtering and reflection of a single N atom and the simultaneous resputtering and reflection of a pair of N atoms. Fig. 3(a) shows that 500 incident atoms randomly impact the different possible adsorption sites of the surface. Meanwhile, the surface atoms are located around different dynamic equilibrium sites after the substrate relaxation. Therefore, it is sound to statistically analyze the atomic interactions between the incident atom and the surface by this simulation. For the convenience of analysis, the distribution of atoms in Fig. 3(a) is contracted into that in Fig. 3(b) by scaling with a_T , where the true coordinate (x_i, y_i) of any atom is transformed into the dimensionless coordinate (x'_i, y'_i) by the following equations:

$$x'_i = x_i - \text{int}(x_i/a_T), \quad y'_i = y_i - \text{int}(y_i/a_T) \quad (2)$$

where the function $\text{int}()$ approximates to the closest smaller integer number. By this transformation method the incident atom distributions in the contraction coordinate systems at different substrate temperatures are plotted in Fig. 3(c)–(f). It can be seen that the initial position distributions of incident atoms occurring different interactions with the substrate surface at different temperatures are similar, indicating these interaction processes preference is independent of the substrate temperature. The impact position plays an important role on determining the interaction modes. The adsorption-favored impact sites are the areas around the surface N atoms marked by the black crosses; the resputtering-favored impact sites are also the areas around but a bit further from the surface N atoms marked by both the blue crosses and the green crosses; other surface sites, especially the positions around the surface Ti atoms, are favored by the reflections marked by both the red crosses and the green crosses. The reflection predominates the interactions, while the adsorption and the reflection have the similar probabilities when $T = 300\text{--}700\text{ K}$ and $E_k = 10\text{ eV}$.

In order to further assess the contribution of each atomic interaction to the impact process of the incident N atom on the TiN(001) surface, for each simulation with 500 separate impact events the number of resputtering processes is compared with that of reflection processes as shown in Fig. 4, where the number of simultaneous resputtering and reflection is also included in the former two numbers. The subfigures at different T are similar, again indicating these interaction processes are independent of the substrate temperature. The resputtering, often accompanied by the reflection resulting in a pair of N atoms leaving off the surface, seldom occurs when E_k is small. Until E_k increases to 10 eV the resputtering gets much active, and the isolated one without accompanying reflection begins to appear, the numbers of which are 2, 0, 9, 1 and 4 for $T = 300, 400, 500, 600$ and 700 K , indicating the little contribution of the isolated resputtering to the impact process. The reflection strengthens significantly with the increase of E_k , and its probability is much larger than that of resputtering. The reflection begins to predominate the interactions when E_k reaches 2 eV, but gets saturated after $E_k = 4\text{ eV}$. The adsorption is the contrary to the resputtering and reflection interactions. Its dependence on T and E_k is discussed via the initial sticking coefficient S_{c0} , which is calculated by equation (1) using the data from Fig. 4. The curves of $S_{c0}\text{--}E_k$ at different temperatures in Fig. 5 irregularly wind each other, indicating the independence of S_{c0} on T . While the effect of E_k on S_{c0} is significant. In order for an incident atom to be adsorbed after colliding with a solid surface, it needs to lose the energy associated with the component of momentum normal to the surface; here for the normal impact the incident atom needs to lose enough of its kinetic energy, resulting in S_{c0} being inversely proportional with E_k . Therefore, S_{c0} decreases sharply from 0.864–0.884 at $E_k = 0.5\text{ eV}$ to 0.16–0.218 at $E_k = 4\text{ eV}$, especially its near-linear change in the region of 1–3 eV completely follows the energy loss assumption above. S_{c0} decreases weakly with E_k after it reaches 4 eV due to the saturation of reflection, and gets 0.17–0.184 at $E_k = 10\text{ eV}$.

3.2. Interactions of incident Ti atoms on the TiN(001) surface

The same simulation procedure is also applied to study the interactions of incident Ti atoms with the TiN(001) surface. The incident Ti atom is observed to be adsorbed on the four-fold hollow site, which is the dynamic equilibrium site of the Ti adatom on the TiN(001) surface proved by another MD study [34]. In current value ranges of T and E_k , the adsorption completely predominates the interactions, and the reflection or resputtering of Ti atoms is not observed. The CMD simulation of Cu atoms impacting the Cu surface indicates that the reflection occurs only when $E_k > 20\text{ eV}$ [35]. Here the maximum value of E_k is 10 eV, which

should be below the low limit of the incident energy activating the Ti reflection. When $E_k \geq 1.5$ eV the resputtering of surface N atoms is observed, but its probability is much smaller than that in the case of the N atoms impacting with the TiN(001) surface. Fig. 6. shows that the number of the resputtered N atoms increases with E_k and reaches a small peak value of 7, indicating the resputtering of N atoms negligible contributing to the interaction, meanwhile it has the weak dependence of T . The initial sticking coefficient of Ti atoms on the TiN(001) surface approximates one, which agrees with the common assumption [23]; it is much larger compared with that of N atoms, indicating that the incident N atom is less apt to be adsorbed on the TiN(001) surface. Therefore, in order to get the stoichiometric TiN film the N/Ti flux ratio should be larger than one and be increased when deposition under high energy.

4. Conclusions

With CMD simulations adopting the 2NN MEAM potentials, the interaction processes between incident N or Ti atoms and the TiN(001) surface are studied under the conditions of normal incidence within the substrate temperature range of 300–700 K and the kinetic energy of incident atoms range of 0.5–10 eV. The results show that the impact of incident N atoms with the surface could result in the N adsorption by the direct impact from the gas phase or by the atomic exchange process, the resputtering of the surface N atom, and the reflection of the incident N atom. The resputtering and reflection may simultaneously occur, resulting in a pair of separate N atoms or a N₂ molecule leaving off the surface. The impact position of incident N atoms on the surface plays an important role in determining the interaction modes. The adsorption-favored sites are the areas around the surface N atoms; the resputtering-favored sites are also the areas around but a bit further from the surface N atoms; other surface areas, especially the positions around the surface Ti atoms, are favored by the reflection. With the increase of the incident energy, the adsorption weakens as the reflection and resputtering strengthen until they reach their own saturated states at different incident energy thresholds. While their occurrence probabilities are independent on the substrate temperature. In the case of the incident Ti atom, adsorption is the predominant interaction mode between particles and the surface. This results in the much smaller initial sticking coefficient of N atoms on the TiN(001) surface compared with that of Ti atoms. To get the stoichiometric TiN film the N/Ti flux ratio should be larger than one and be increased with the higher incident energy.

Acknowledgments

This work was supported by grants from the China Postdoctoral Science Foundation (Grant No. 2013M540277), Heilongjiang Postdoctoral Fund (Grant No. LBH-Z13089), Natural Scientific Research Innovation Foundation in Harbin Institute of Technology (Grant No. HIT.NSRIF.2015006), and the Seventh Framework Program of the European Community for Research (Grant No. CP-FP 213600-2 M3-2S).

References

- [1] G. Bartarya, S.K. Choudhury, State of the art in hard turning, *Int. J. Mach. Tools Manuf.* 53 (2012) 1–14.
- [2] F. Lang, Z. Yu, The corrosion resistance and wear resistance of thick TiN coatings deposited by arc ion plating, *Surf. Coat. Technol.* 145 (2001) 80–87.
- [3] N. Vershinin, K. Filonov, B. Straumal, W. Gust, I. Wiener, E. Rabkin, A. Kazakevich,

- Corrosion behaviour of the protective and decorative TiN coatings on large area steel strips, *Surf. Coat. Technol.* 125 (2000) 229–232.
- [4] Y. Shin, Y. Shimogaki, Diffusion barrier property of TiN and TiN/Al/TiN films deposited with FMCVD for Cu interconnection in ULSI, *Sci. Technol. Adv. Mater.* 5 (2004) 399.
 - [5] N.Y. Kim, Y.B. Son, J.H. Oh, C.K. Hwangbo, M.C. Park, TiN_x layer as an antireflection and antistatic coating for display, *Surf. Coat. Technol.* 128-129 (2000) 156–160.
 - [6] V. Pham, S. Jun, H. Kim, Y. Koh, Deposition of titanium nitride (TiN) on Co–Cr and their potential application as vascular stent, *Appl. Surf. Sci.* 258 (2012) 2864–2868.
 - [7] S. Mahieu, D. Depla, Reactive sputter deposition of TiN layers: modelling the growth by characterization of particle fluxes towards the substrate, *J. Phys. D Appl. Phys.* 42 (2009) 053002.
 - [8] T. Giela, K. Freindl, N. Spiridis, J. Korecki, Au(1 1 1) films on W(1 1 0) studied by STM and LEED – Uniaxial reconstruction, dislocations and Ag nanostructures, *Appl. Surf. Sci.* 312 (2014) 91–96.
 - [9] D.G. Sangiovanni, D. Edström, L. Hultman, V. Chirita, I. Petrov, J.E. Greene, Dynamics of Ti, N, and TiN_x ($x=1-3$) ad molecule transport on TiN(001) surfaces, *Phys. Rev. B* 86 (2012) 155443.
 - [10] I. Petrov, A. Myers, J.E. Greene, J.R. Abelson, Mass and energy resolved detection of ions and neutral sputtered species incident at the substrate during reactive magnetron sputtering of Ti in mixed Ar+N₂ mixtures, *J. Vac. Sci. Technol. A* 12 (1994) 2846–2854.
 - [11] K. Wegner, P. Piseri, H.V. Tafreshi, P. Milani, Cluster beam deposition: a tool for nanoscale science and technology, *J. Phys. D Appl. Phys.* 39 (2006) R439–R459.
 - [12] Z.H. Xu, L. Yuan, D.B. Shan, B. Guo, A molecular dynamics simulation of TiN film growth on TiN(001), *Comput. Mater. Sci.* 50 (2011) 1432–1436.
 - [13] S. Zhang, H. Gong, X. Chen, G. Li, Z. Wang, Low energy Cu clusters slow deposition on a Fe (001) surface investigated by molecular dynamics simulation, *Appl. Surf. Sci.* 314 (2014) 433–442.
 - [14] H.N. Wadley, X. Zhou, R.A. Johnson, M. Neurock, Mechanisms, models and methods of vapor deposition, *Progress Mater. Sci.* 46 (2001) 329–377.
 - [15] X.W. Zhou, D.A. Murdick, B. Gillespie, H.N.G. Wadley, Atomic assembly during GaN film growth: Molecular dynamics simulations, *Phys. Rev. B* 73 (2006) 045337.
 - [16] H. Chen, A.K. Tieu, Q. Liu, I. Hagiwara, C. Lu, Molecular dynamics simulation about porous thin-film growth in secondary deposition, *Appl. Surf. Sci.* 253 (2007) 7471–7477.
 - [17] T.B. Ma, Y.Z. Hu, H. Wang, Growth of ultrathin diamond-like carbon films by C₆₀ cluster assembly: Molecular dynamics simulations, *Diam. Relat. Mater.* 18 (2009) 88–94.
 - [18] S.F. Hwang, Y.H. Li, Z.H. Hong, Molecular dynamic simulation for Cu cluster deposition on Si substrate, *Comput. Mater. Sci.* 56 (2012) 85–94.
 - [19] D. Gall, S. Kodambaka, M.A. Wall, I. Petrov, J.E. Greene, Pathways of atomistic processes on TiN(001) and (111) surfaces during film growth: an *ab initio* study, *J. Appl. Phys.* 93 (2003) 9086–9094.
 - [20] D. Edström, D.G. Sangiovanni, L. Hultman, I. Petrov, J.E. Greene, V. Chirita, The dynamics of TiN_x ($x=1-3$) ad molecule interlayer and intralayer transport on TiN/TiN(001) islands, *Thin Solid Films* 589 (2015) 133–144.
 - [21] G. Armand, J.R. Manson, Sticking coefficient of light particles on surfaces, *Phys. Rev. B* 43 (1991) 14371–14377.
 - [22] L. Schwaederlé, P. Brault, C. Rond, A. Gicquel, Molecular Dynamics Calculations of CH₃

- Sticking Coefficient onto Diamond Surfaces, *Plasma Process. Polym.* 12 (2015) 764–770.
- [23] D. Mao, J. Hopwood, Ionized physical vapor deposition of titanium nitride: A deposition model, *J. Appl. Phys.* 96 (2004) 820–828.
- [24] J.F. Ziegler, J.P. Biersack, U. Littmark, *The Stopping and Range of Ions in Matter*, Pergamon, New York, 1985.
- [25] Y.M. Kim, B.J. Lee, M.I. Baskes, Modified embedded-atom method interatomic potentials for Ti and Zr, *Phys. Rev. B* 74 (2006) 014101.
- [26] B. Lee, T. Lee, S. Kim, A modified embedded-atom method interatomic potential for the Fe-N system: A comparative study with the Fe-C system, *Acta Mater.* 54 (2006) 4597–4607.
- [27] M. Ohring, *Materials Science of Thin Films: Deposition and Structure*, 2nd ed., Academic Press, London, 2001.
- [28] S.J. Plimpton, Fast parallel algorithms for short-range molecular dynamics, *J. Comput. Phys.* 117 (1995) 1–19.
- [29] J. Li, AtomEye: an efficient atomistic configuration viewer, *Model. Simul. Mater. Sci. Eng.* 11 (2003) 173–177.
- [30] D.G. Sangiovanni, D. Edströma, L. Hultman, I. Petrov, J.E. Greene, V. Chirita, *Ab initio* and classical molecular dynamics simulations of N₂ desorption from TiN(001) surfaces, *Surf. Sci.* 624 (2014) 25–31.
- [31] X.W. Zhou, H.N. Wadley, Atomistic simulations of the vapor deposition of Ni/Cu/Ni multilayers: The effects of adatom incident energy, *J. Appl. Phys.* 84 (1998) 2301–2315.
- [32] M.I. Haftel, M. Rosen, T. Franklin, M. Hettermann, Molecular dynamics observations of interdiffusion and Stranski-Krastanov growth in the early film deposition of Au on Ag(110), *Phys. Rev. Lett.* 72 (1994) 1858–1861.
- [33] M.I. Haftel, M. Rosen, T. Franklin, M. Hettermann, Molecular-dynamics investigation of early film growth of Pt/Au(100) and Au/Pt(100) and an interdiffusive growth mode, *Phys. Rev. B* 53 (1996) 8007–8014.
- [34] D.G. Sangiovanni, D. Edströma, L. Hultman, I. Petrov, J.E. Greene, V. Chirita, Ti adatom diffusion on TiN(001): *Ab initio* and classical molecular dynamics simulations, *Surf. Sci.* 627 (2014) 34–41.
- [35] X.W. Zhou, H.N. Wadley, Hyperthermal vapor deposition of copper: reflection and resputtering effects, *Surf. Sci.* 431 (1999) 58–73.

Figures

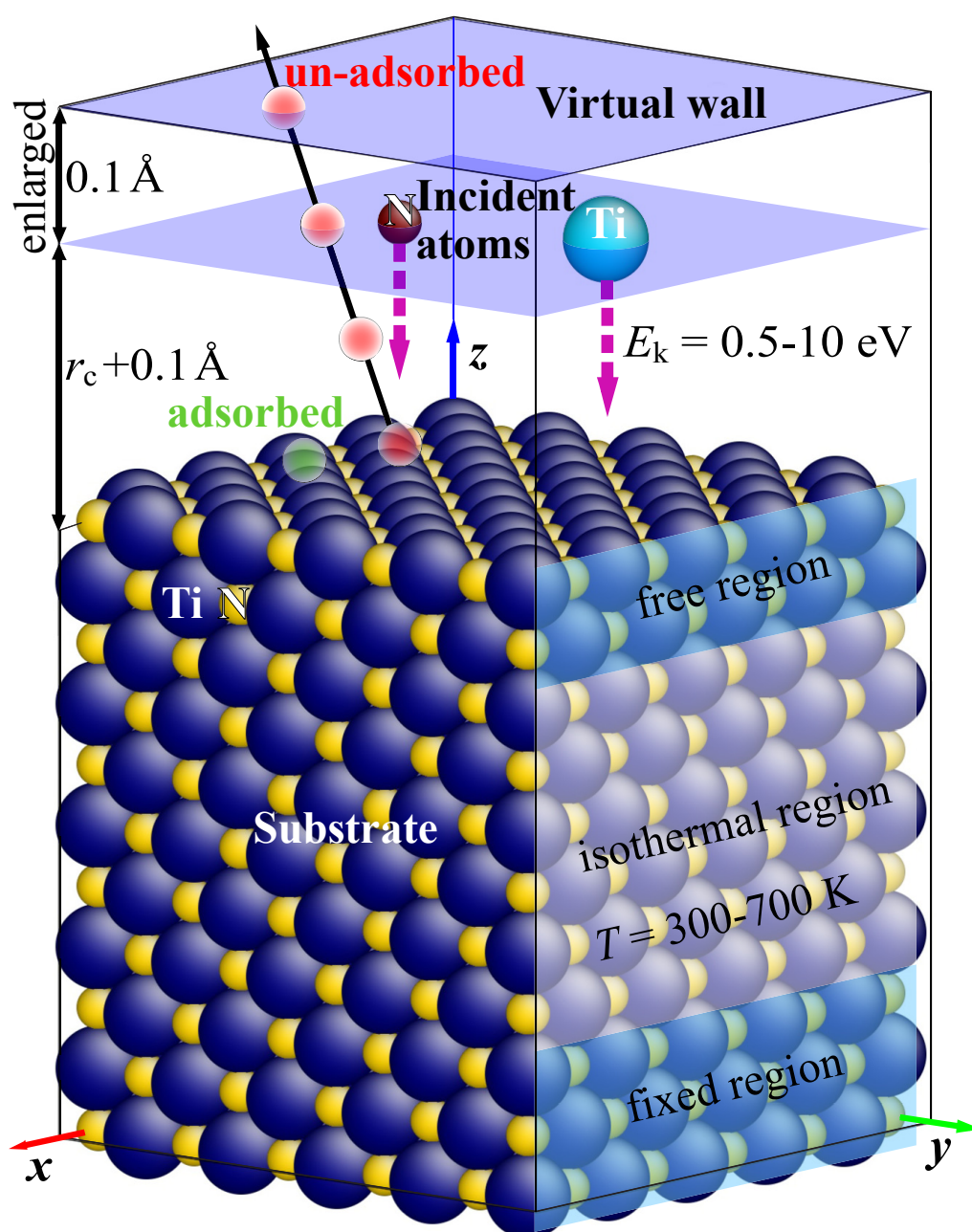


Fig. 1. CMD model of the impact of incident N or Ti atoms against the TiN(001) surface.

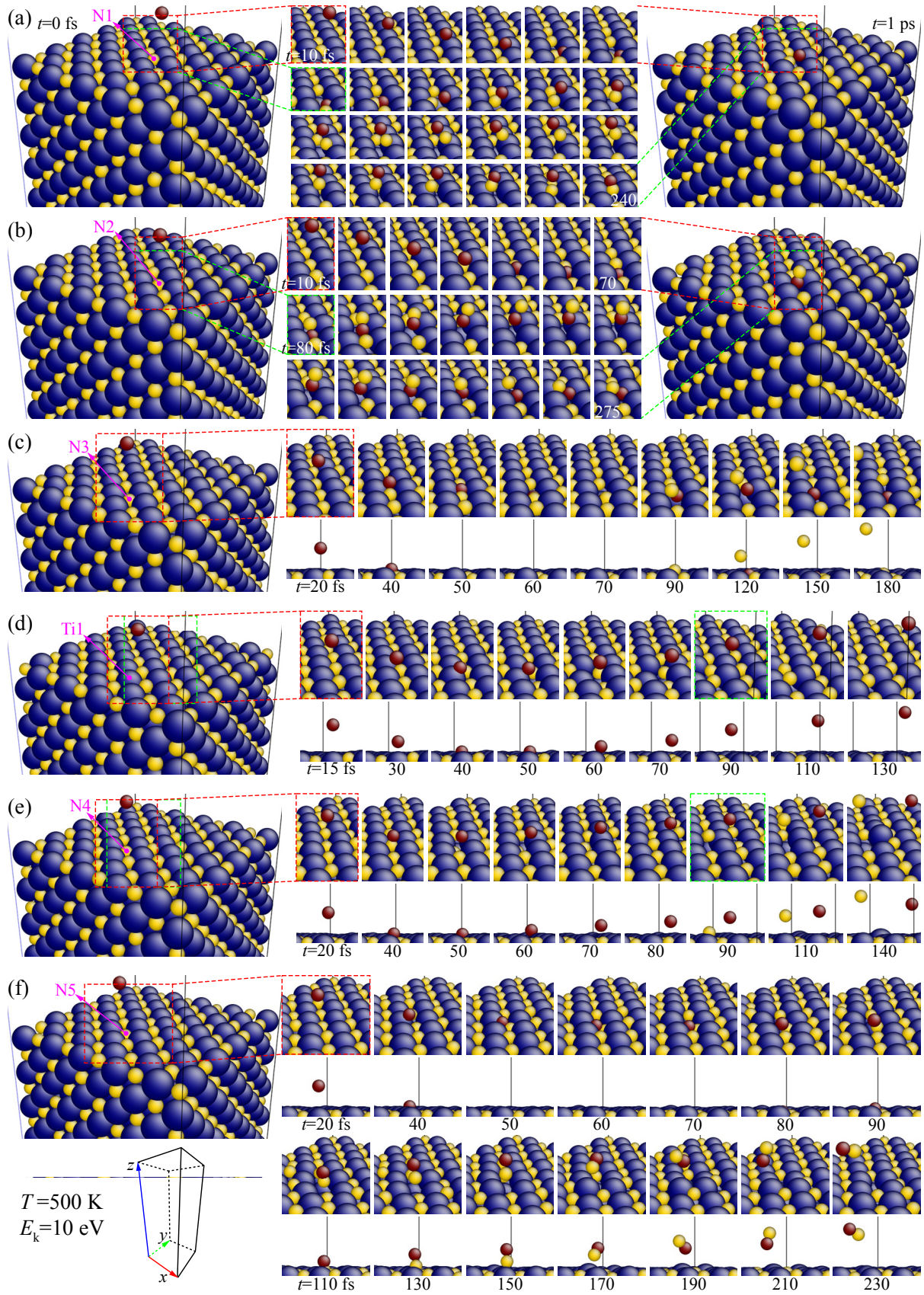


Fig. 2. Time-resolved interaction processes between incident N atoms and TiN(001) surfaces at $T = 500$ K and $E_k = 10$ eV (see also Supplementary Animations 1–6): N adsorption by the direct impact from the gas phase (a) or by the atomic exchange mechanism (b); (c) resputtering of the surface N atom; (d) reflection of the incident N atom; simultaneous reflection and resputtering resulting in a pair of separate N atoms (e) or a N_2 molecule (f) leaving off the surface.

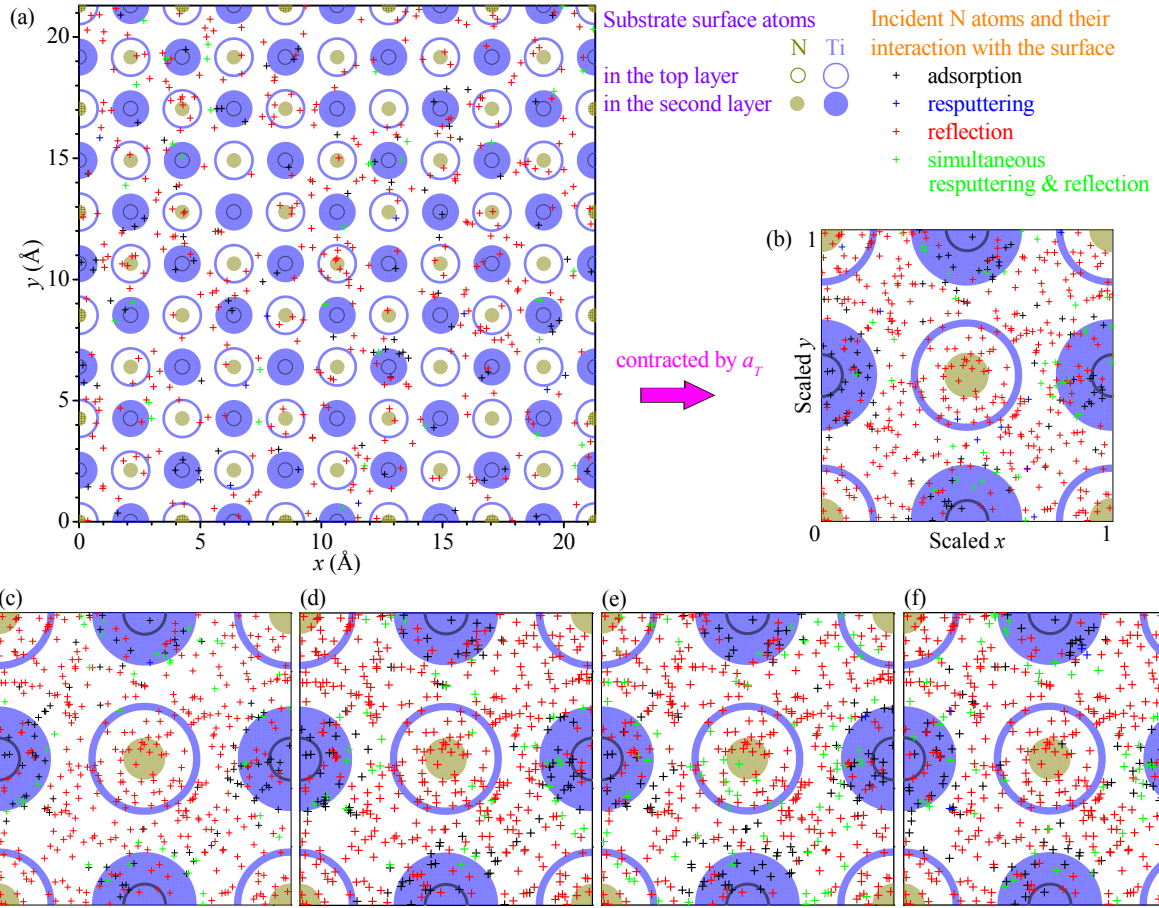


Fig. 3. Initial position distributions of the incident N atoms occurring different interactions with the TiN(001) surfaces: in the true coordinate system at $T = 500$ K (a); in the contraction coordinate system at $T = 500$ K (b), $T = 300$ K (c), $T = 400$ K (d), $T = 600$ K (e) and $T = 700$ K (f).

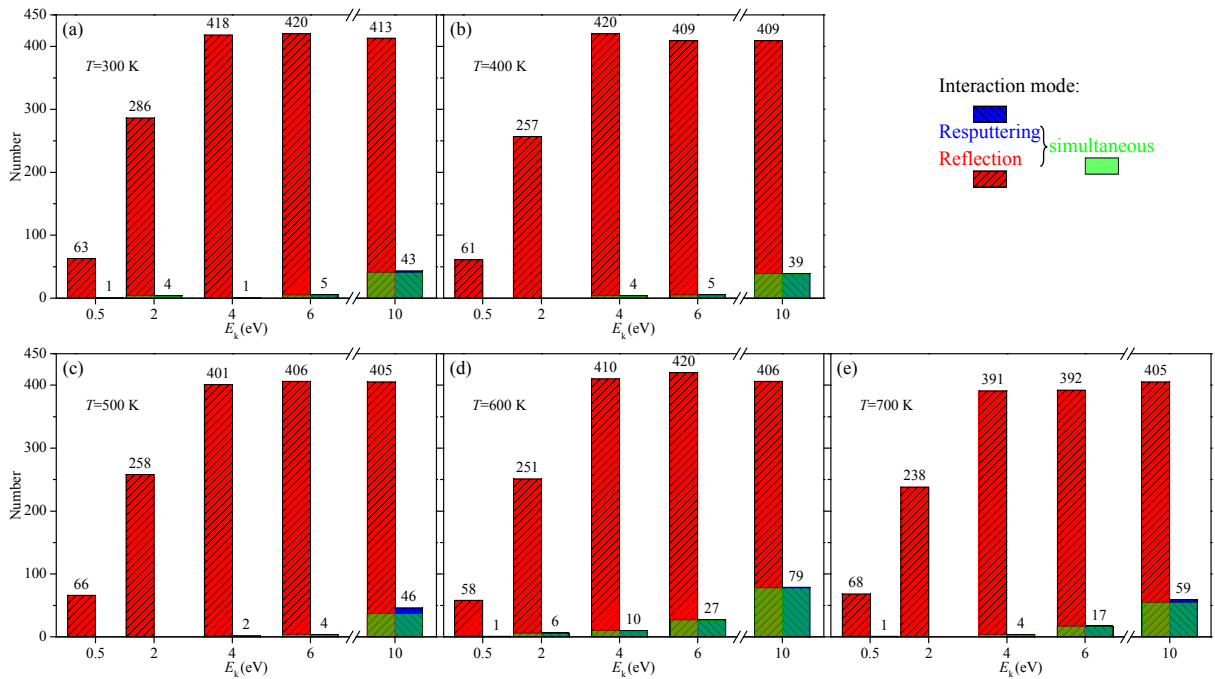


Fig. 4. Variations of the number of resputtering processes and that of reflection processes with T and E_k : (a) $T = 300$ K, (b) $T = 400$ K, (c) $T = 500$ K, (d) $T = 600$ K and (e) $T = 700$ K.

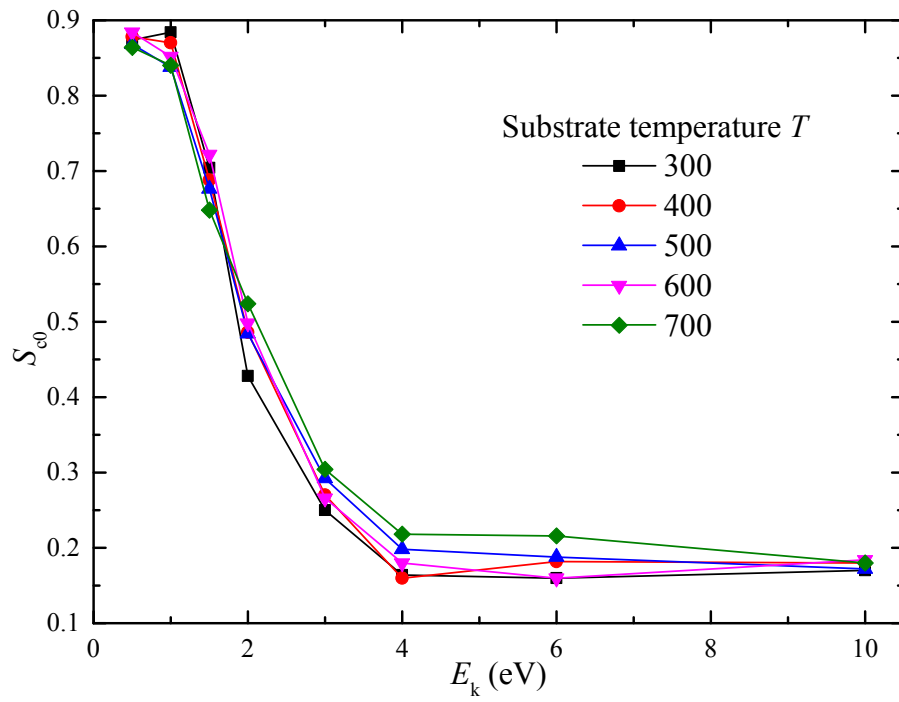


Fig. 5. Variations of S_{e0} of the atomic N on the TiN(001) surface with T and E_k .

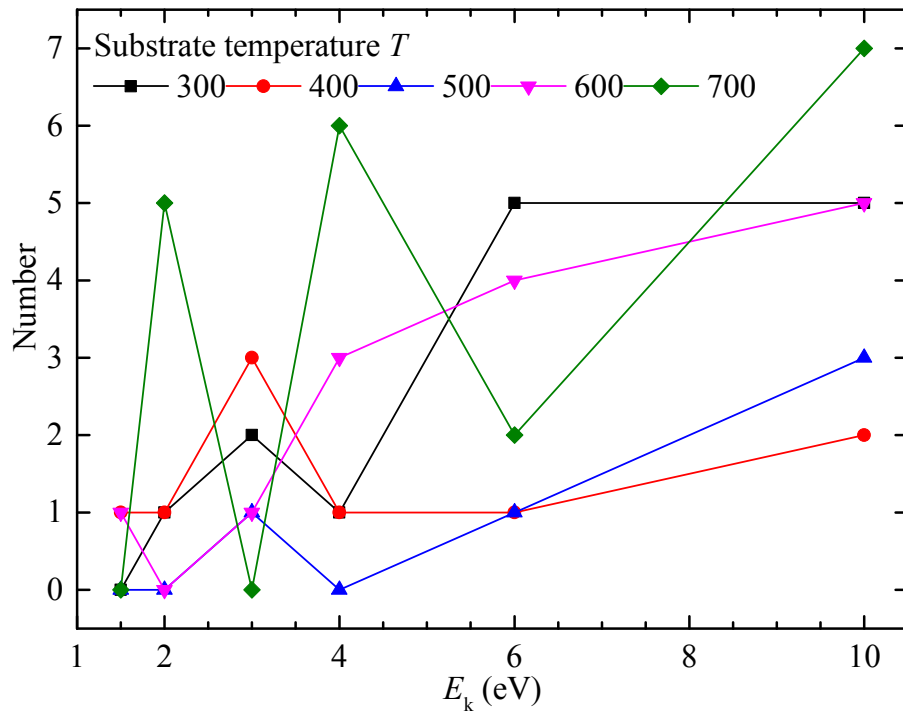


Fig. 6. Variations of the number of the resputtered N atoms with T and E_k .

Supplementary materials

Supplementary Animation 1. N adsorption by the direct impact from the gas phase.

Supplementary Animation 2. N adsorption by the atomic exchange.

Supplementary Animation 3. Resputtering of the surface N atom.

Supplementary Animation 4. Reflection of the incident N atom.

Supplementary Animation 5. Simultaneous resputtering and reflection resulting in a pair of separate N atoms leaving off the surface.

Supplementary Animation 6. Simultaneous resputtering and reflection resulting in a N₂ molecule leaving off the surface.

Supplementary data associated with this article can be found, in the online version, at <http://dx.doi.org/10.1016/j.apsusc.2015.11.090>.

Highlights

Interactions of incident N or Ti atoms with TiN(001) surface are studied by CMD.

The impact position of incident N on the surface determines the interaction modes.

Adsorption could occur due to the atomic exchange process.

Resputtering and reflection may simultaneously occur.

The initial sticking coefficient of N on TiN(001) is much smaller than that of Ti.

Time-resolved **interaction** processes of incident N atoms with TiN(001) surfaces at $T=500$ K and $E_k=10$ eV

